Water Air Soil Pollut (2007) 178:179–193
DOI 10.1007/s11270-006-9189-8

Hydrogeochemistry and Water Balance in the Coastal Wetland Area of "Biviere di Gela," Sicily, Italy

Emanuela Manno · Massimo Vassallo · Daniela Varrica · Gaetano Dongarrà · Sergio Hauser

Received: 2 February 2006 / Accepted: 20 May 2006 / Published online: 28 July 2006

Abstract In the study area physical and chemical factors control the composition of surface and groundwaters, which in turn determine the water quality of the "Biviere di Gela" lake. These factors combine to create diverse water types which change their compositional character spatially as rainfall infiltrates the soil zone, moves down a topographically defined flow path, and interacts with bedrock minerals. Low-salinity waters, which represent the initial stage of underground circulation, start dissolving calcium carbonate from the local rocks. The progressive increase in salinity, characterized by substantially higher Ca, SO_4, Na and Cl concentrations, suggests that dissolution of $CaSO_4$ and NaCl is an important process during water–rock interactions. The "Biviere di Gela" lake is often separated into two units (Lago Grande and Lago Piccolo). "Lago Grande" water is generally of Na-SO_4-Cl-type, whereas "Lago Piccolo" water is of Na-Cl-SO_4-type. Their total content of dissolved salts varies with season, the amount of rainfall, and inflow of ground and drainage water. Over time, an increasing trend towards greater salinity and also sudden changes in the relative abundances of Cl and SO_4 have been recorded for the "Lago Grande." The isotope composition of the lake water appears to be affected by inflow of ground and surface waters and also by evaporative loss. The nitrate content of waters from the recharge basin is of particular concern because it contributes to lake eutrophication. The trace element contents do not evidence the presence of any significant metal contamination of lake waters, although a future potential hazard of metals bioaccumulation by the aquatic biota must be taken into consideration. Finally, a water balance for the basin shows that a drop in precipitation of about 20% might be critical for lake survival.

Keywords wetland area · hydrogeochemistry · environmental geochemistry · isotope geochemistry · water balance

1 Introduction

Wetlands are peculiar environments of fundamental importance for the conservation of biodiversity, since they support high numbers of different plants, birds, mammals, reptiles, amphibians, fish and invertebrate species. Water quality is one of the most important factors controlling the ecological processes which make wetlands among the world's most productive environments. The "Biviere di Gela" lake is the largest natural coastal lake in Sicily (120 ha) and one of the few natural wetlands left on the island. Being the habitat of many species of animals and

---

E. Manno · M. Vassallo · D. Varrica ·
G. Dongarrà (✉) · S. Hauser
Dipartimento di Chimica e Fisica della Terra (C.F.T.A.),
Università di Palermo, via Archirafi 36,
90123 Palermo, Italy
e-mail: dongarra@unipa.it

plants, including very rare and endangered species, in order to promote its conservation it has been designated for the List of Wetlands of International Importance. The lake has brackish water, with a degree of salinity which varies according to season, amount of rainfall, and inputs of ground and drainage water. The wetland falls within the territory of Gela, which is characterized by potential polluting sources such as a petro-chemical plant, located only a few kilometres away, and widespread greenhouse cultivation in the surrounding area. For this reason, it has been defined as an “area with high risk of environmental collapse.” Its water geochemistry is therefore influenced by several factors which include: a) type of rocks present and intensity of water-rock interactions; b) removal processes of aquatic species; c) evaporation processes; d) anthropic activities.

A geochemical survey to establish the principal chemical processes controlling lake water quality was considered necessary to promote environmental protection, preservation and recovery of this ecological system. Therefore, as well as the lake waters, it was decided to study the chemical and isotope composition of the groundwaters of the recharge basin, in order to define their origin and the main geochemical reactions responsible for the quality of the groundwater feeding the lake. Samples of lake sediments were also examined.

2 Experimental

2.1 Site description

The wetland area (37°01′20″N, 01°53′30″E) studied here is located in SE Sicily (Italy), 10 km SE of the town of Gela, 1.5 km from the Mediterranean coast and 8 m a.s.l. (Figure 1). It is characterized by low hills running NE-SW, with a maximum altitude of 694 m and a mean value of 336 m. Their continuity is interrupted by buried faults going back to the last tectonic phases of the Quaternary, thus influencing the hydrographic network. The lake has a NW-SE running elliptical form with a surface area of approximately 1.2 km^2, a maximum depth of about 8 m, and a water volume of about 5.8 × 10^6 m^3 (GreenStream, 2003). It has no surface outflow and no important inflow, being fed during the rainy season by an ephemeral surface stream (Valle Torta) and from an artificial canal downstream of the Dirillo dam. Water losses from the lake include evaporation from the water surface and underground outflow to down-gradient groundwater. When the water level is less than 1.6 m, the lake separates into two units (Lago Grande to the east, and Lago Piccolo to the west). Since 1952, a decrease in the lake volume has been observed, probably due to solid transport of surface runoff.

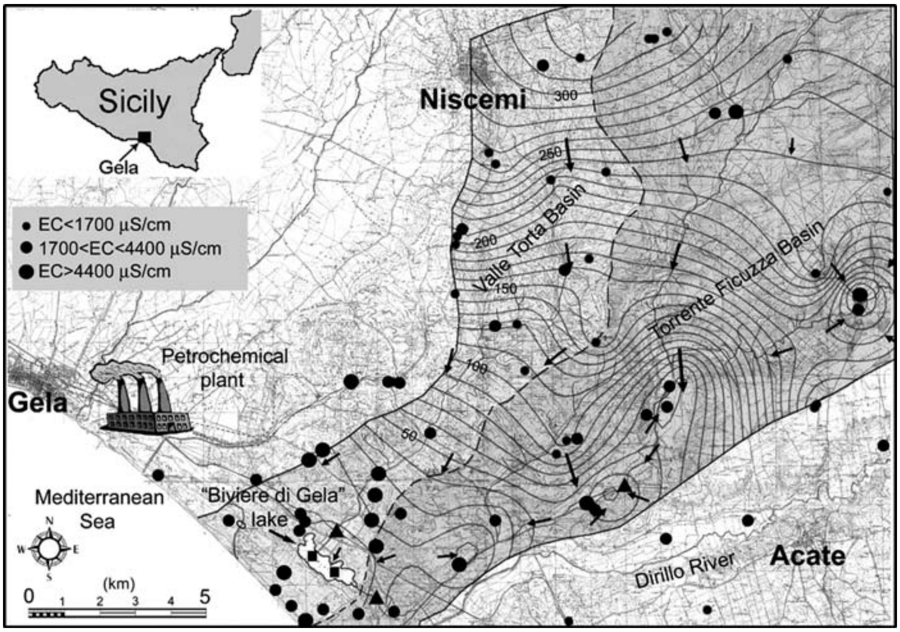

Figure 1 Location of the study area and sampling points of groundwaters (●), streams (▲) and lake water (■). The isopiezometric contours are drawn from data of April 2004.

The study area presents typical Mediterranean conditions, with mild, relatively rainy winters and warm, dry summers. The air temperature ranges from 11 to 29°C and the average annual rainfall is 373 mm/year (data from Servizio Idrografico del Genio Civile, 1980–2000). Almost 70% of total annual rainfall occurs between September and February. Prevailing winds, generally breezes, are from the NE and SE sectors. The aridity index (De Martonne, 1926) computed for the Hyblean coastal area is less than 15, and therefore classifies the area as semi-arid.

2.2 Geology and hydrogeology

From a geological point of view, the study area belongs to the Late Quaternary morphological element named "Piana di Gela," and is located in the transitional zone towards the foredeep or "Caltanissetta" basin, at the edge of the Hyblean Plateau. The "Piana di Gela" originated from the complex interplay of tectonic events with eustatic sea-level changes (Pedley & Grasso, 1991). The abrasive action of the sea eroded the highly deformed Mio-Pliocene terrains of the Gela Nappe, leaving clayey–sandy deposits during the drop in sea level (Butler, Grasso, & Lickorish, 1995a; Butler, Lickorish, Grasso, Pedley, & Ramberti, 1995b; Butler, McClelland, & Jones, 1999; Roda, 1966).

The area is covered by Neogene and Quaternary deposits. The former are made up of clay, marly clay and evaporitic deposits in the lower part, and marly limestone in the upper part. The Quaternary deposits are made up of sandy clays in the lower part which gradually changes to yellow sand, conglomerates and sandy limestone in the upper part. The latter are extensive although not thick. Alluvial deposits are found along the main streams. There are also clayey-silt lacustrine deposits near the lake. The Messinian–Pleistocene terrains, made up of clayey deposits and characterized by chaotic texture, contain resedimented gravel of various ages composed of gypum, clay, sandstone, Mesozoic limestone and, sporadically, basalt (Beneo, 1949).

Based on the hydraulic conductivity of the main lithotypes, the following hydrogeologic complexes are distinguished:

- Clayey–silty–lacustrine complex, less than 10 m thick and characterized by low permeability;
- Alluvial complex, of variable thickness and permeability, depending on prevailing lithologies;
- Sandy and sandy–clayey complex, of high permeability where sandy terms prevail and low permeability where clayey terms prevail;
- Marl–clayey complex, representing the impervious substrate of the Pleistocene aquifer;
- Evaporitic complex, of elevated permeability;
- Marl–clayey complex of Tortonian age, of very low permeability.

On the whole, the area is characterized by a single aquifer system, with local semi-confined layers, overlying the impermeable clay basement. Piezometric measurements (Figure 1) have shown that the main groundwater flow is from NE to SW, and that the top of the water table is at about 2 m. The observed increase in hydraulic gradient near some wells and the Ficuzza river suggests conspicuous over-exploitation of the aquifer in this area. Even near the lake, the piezometric level seems to be influenced by over-exploitation, which causes it to fall below sea level. Nevertheless, seawater intrusion along the coast is severely limited by the presence of the impervious marl–clayey complex.

A simplified water balance for the basin (279 km^2) has been calculated. Evapotranspiration (E_{tr}), computed using the classical method of Thornthwaite (1948) amounts to 307 mm/year. Taking into account the estimated monthly potential evapotranspiration and rainfall (373 mm/year), meteoric recharge into the aquifer is restricted to a few months during autumn–winter.

In the study area, the amount of infiltrated water has been estimated in about 59 mm/year, which corresponds to a potential water supply of 17×10^6 m^3/year. More than 71% of this supply (12×10^6 m^3/year) is used for the requirements of greenhouse cultivation (data from ISTAT, 2000). Surface drainage is very limited (1.8×10^6 m^3/year), due to the limited topographic gradient and to deposits of high hydraulic conductivity.

A simple quantitative water balance of the lake, for a fixed time interval, may be written as:

$$\Delta V = V_p + V_{gi} + V_s - V_e - V_{go}$$

where:

ΔV Change in volume
V_p Precipitation (0.40×10^6 m^3/year)

V_{gi} Groundwater input (0.005×10^6 m^3/year)
V_s Surface runoff from Valle Torta Basin and the artificial canal downstream of the Dirillo dam (1.90×10^6 m^3/year)
V_e Evaporation (0.75×10^6 m^3/year)
V_{go} Groundwater outflow (0.003×10^6 m^3/year)

The imbalance between precipitation and evaporation rates determines a hydrological deficit in the lake budget, mainly compensated by surface runoff. Measured data imply that, during summer, the lake feeds the nearby groundwater table. Water input variations have considerable effects on the lake water level and on the ecological conditions. It is worth noting that a drop in precipitation of about 20% would become critical in maintaining the present water level and might be critical for lake survival.

2.3 Sampling and analytical methods

A total of 134 samples of groundwaters (128) and streams (6) from the catchment area were collected from 70 sampling points on July 2003, April 2004 and November 2004. Lake water samples were collected 11 times, approximately 0.5 m below the surface. The locations of water sampling points are shown in Figure 1. Rainwater samples for stable isotope measurements were collected on a monthly basis from August 2003 to February 2005 at the rain station located inside the study area at 11 m a.s.l. All samples were filtered through 0.45 μm Millipore MF filters and stored in pre-washed polypropylene bottles. Field measurements included the depths of wells, water temperature, pH, electrical conductivity (EC), Eh and dissolved O_2. Major cations and anions, including Ca, K, Na, Mg, Br, Cl, F, NO_3 and SO_4, were analysed by Dionex 300 ion chromatograph, with precision better than ±5%. Inductively coupled mass spectrometry (ICP-MS, Perkin Elmer, Elan 6100 DRC-e) was used to determine Sr. SiO_2 was determined spectrophotometrically, and HCO_3 and CO_3 by titration with 0.1 N HCl. Total dissolved solid (TDS) contents were calculated from the electrical conductivity values by Aquachem software.

Dissolved trace elements were analysed by ICP-MS after addition of rhenium–scandium–yttrium as internal standards. The accuracy of the analyses (±10%) was assessed by running the SRM-1640, a simulated groundwater sample for trace metals.

Oxygen and hydrogen stable isotope ratios are reported in terms of δ units (per mille deviation of isotope ratios from international standard V-SMOW). The overall precision of isotope determination was 1‰ and 0.1‰ for δ^2H and δ^{18}O, respectively.

Trace elements in bulk lake sediments (<63 μm) were also determined by ICP-MS, after digestion with a mixture 3:2:1 of HNO_3–$HClO_4$–HF in teflon vessel and heated in microwave system (CEM).

Leaching tests were performed on samples of the main lithotypes present in the study area. 100 g of finely powdered samples were shaken at room temperature for 48 h with 200 ml of ultrapure 18 MΩ water. The extract solution were filtered and analysed for major elements as above.

WATEQ4F software (Ball & Nordstrom, 1991) was used to calculate the thermodynamic equilibrium conditions of groundwaters with respect to the main mineral phases present in the aquifer. Saturation indices were calculated using ion activities as follows SI = Log(IAP/Kt), where IAP is the ion activity product of the solution and Kt is the equilibrium constant at the temperature measured.

3 Results and Discussion

3.1 Groundwater chemistry

A univariate overview of major chemical compositions, including standard deviations and variation coefficients, is listed in Table I. Since small variations in time were observed in the concentration values, spatial distribution is probably the main controller of variations in the data. As may be seen, groundwater temperatures range between 14 and 28°C, thus indicating the shallow nature of the aquifer system. pH values are close to neutrality, and EC and TDS in groundwater samples range from 610 to 7,620 μS/cm and 406 to 6,367 mg/l, respectively.

The calculated saturation indexes (SI) show that most water samples are saturated with respect to calcite, aragonite, dolomite and barite, but undersaturated with respect to gypsum, amorphous silica and fluorite. The degree of undersaturation with respect to gypsum decreases with increasing total salinity.

The chemical variables related to total dissolved species exhibit high variation coefficients, revealing great variability in both salinity and ion composition.

Table I Descriptive statistics of physico-chemical parameters and element concentrations in groundwaters and average chemical composition of stream waters

		T	pH	Eh	O_2	EC	TDS	Na	K	Mg	Ca	Sr	SiO_2	F	Cl	Br	NO_3	SO_4	CO_3	HCO_3	P_{CO2}	$\delta^{18}O$	δD
Groundwaters	Number of cases (128)																						
	Mean	19	7.3	150	4.8	2,706	1,670	283	16	73	190	3.0	20	1.0	494	10	82	359	0.2	275	8.3E-04	−4.9	−29
	Minimum	14	6.7	−573	0.6	610	406	26	1.7	6.8	50	0.4	0.8	0.1	36	0.1	0.5	1.7	0.03	107	1.3E-05	−6.1	−38
	Maximum	28	8.7	282	17	7,620	6,367	1,493	108	325	536	8.4	42	12	2,607	70	482	1,280	1.3	546	5.8E-03	−1.5	−12
	SD	2.7	0.4	122	2.6	1,780	1,091	276	20	62	96	2.0	6.4	1.3	492	14	92.4	278	0.2	87	9.0E-04	0.8	4
	CV%	14	5	82	54	66	65	97	129	84	50	66	33	139	99	139	112	77	105	31	108	−16	−13
Streams	Number of cases (2)																						
	Dirillo	14	8.1	156	9.4	1,871	1,434	91	10	45	259	4.3	17	0.6	133	1.7	25	669	0.6	193	8.4E-05	−4.8	−28
	Valle Torta	13	8.1	198	8.5	2,338	1,385	214	9.4	67	185	3.9	17	1.0	349	4.5	24	430	0.9	266	1.0E-04	−5.0	−27
	Ficuzza	15	8.3	182	8.8	1,810	1,038	169	8.7	59	126	1.9	15	1.1	265	3.3	13	341	1.1	216	9.5E-05	−5.0	−29

T: Temperature (°C), EC: Electrical conductivity (μS/cm); Eh (mV), P_{CO2} (atm), $\delta^{18}O$ and δD in per mille (‰) vs V-SMOW; TDS, O_2 and ionic concentrations in milligram per liter (mg/L). SD indicates the standard deviation and CV% the variation coefficient defined as 100 × SD/mean.

They also indicate that the groundwater in the area is not uniform, but may change considerably from one part of the basin to another.

3.2 Statistical treatment of data

The frequency distribution of EC values in the water samples (Figure 2) indicates that the population is made up of three subpopulations: One with a modal peak at 1,050 μS/cm, a second with a peak at 2,450 μS/cm, and the third with a larger value of 5,250 μS/cm. The inflection points in the S-shaped cumulative frequency curve (Tennant & White, 1959) at EC values of 1,700 μS cm^{-1} and 4,400 μS cm^{-1} conveniently distinguish the three subpopulations, according to total contents of dissolved solids. Significant differences ($P < 0.05$) among the groups were also found for almost all the other examined variables. Descriptive statistics for the physico-chemical properties of each subpopulation are listed in Table II.

A cluster analysis, using the Pearson *r*-correlation coefficient, was applied to 14 variables from the obtained data. Figure 3 shows the dendrogram structure produced by the clustering procedure. At

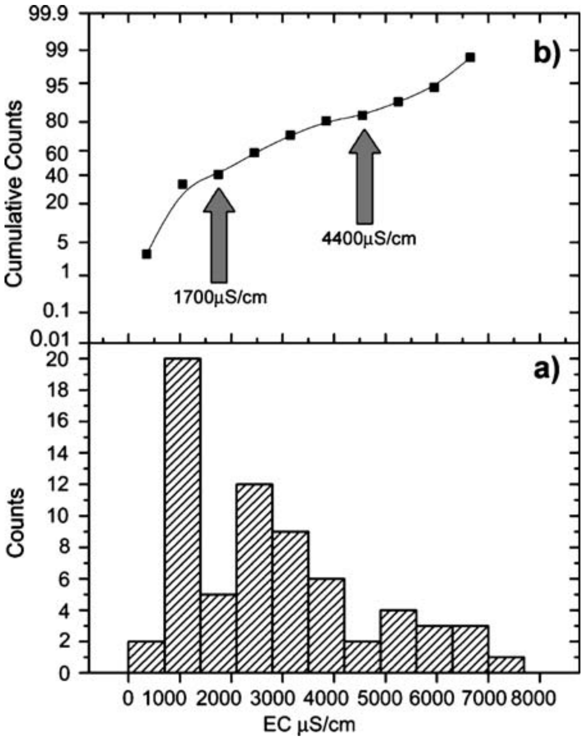

Figure 2 (a) Distribution of measured EC values and (b) cumulative frequency. The break points (*arrows*) separate three

Table II Descriptive statistics of physico-chemical parameters and element concentrations in the three groundwater subpopulations

		T	pH	Eh	O_2	EC	TDS	Na	K	Mg	Ca	Sr	SiO_2	F	Cl	Br	NO_3	SO_4	CO_3	HCO_3	P_{CO2}	$\delta^{18}O$	δD
EC<1,700 µS/cm	Number of cases	24	24	20	20	24	24	24	24	24	24	24	24	24	24	24	24	24	24	24	24	24	24
	Mean	20	7.5	127	4.9	1,066	738	65	5.3	23	107	1.3	19	0.5	118	1.7	35	121	0.2	235	5.E-04	−5.3	−31
	Minimum	16	7.0	−573	0.6	610	473	26	2.0	7.3	61	0.0	14	0.2	36	0.3	1.1	41	0.1	155	7.E-05	−5.7	−34
	Maximum	24	8.1	257	7.9	1,542	1,073	128	26	64	176	5.4	25	0.7	239	8.3	116	296	0.8	374	1.E-03	−4.8	−30
	SD	2.0	0.3	195	2.4	250	162	26	5.0	13	31	1.2	3.0	0.1	48	1.8	34	69	0.2	52	3.E-04	0.3	1
	CV%	10	4	153	50	23	22	40	94	59	29	90	16	23	41	107	98	57	82	22	64	−5	−4
1,700<EC>4,400 µS/cm	Number of cases	30	30	26	26	30	30	30	30	30	30	30	30	30	30	30	30	30	30	30	30	30	30
	Mean	19	7.3	174	5.0	2,897	1,828	276	17	82	222	3.4	20	1.1	481	11	90	447	0.2	291	1.E-03	−4.6	−28
	Minimum	14	6.7	−66	2.1	1,822	976	100	2.4	26	125	0.0	4.8	0.2	167	1.3	9.4	110	0.0	138	7.E-05	−5.9	−36
	Maximum	26	8.1	256	10.8	4,030	2,631	486	76	147	337	6.6	36	2.6	766	42	213	731	1.0	530	4.E-03	−1.5	−12
	SD	2.3	0.3	62	2.1	647	421	112	18	32	57	1.6	7.8	0.7	178	11	71	174	0.2	88	8.E-04	0.9	5
	CV%	13	5	36	41	22	23	40	110	39	26	44	39	61	37	98	79	39	104	30	83	−19	−16
EC>4,400 µS/cm	Number of cases	13	13	10	10	13	13	13	13	13	13	13	13	13	13	13	13	13	13	13	13	13	13
	Mean	21	7.0	97	3.8	5,766	3,355	740	30	162	298	4.8	23	1.9	1,311	21	111	693	0.1	339	1.E-03	−4.5	−28
	Minimum	19	6.8	−85	1.2	4,660	2,365	501	6.1	74	106	0.0	17	0.1	845	4.9	0.6	51	0.1	228	5.E-04	−5.2	−31
	Maximum	24	7.4	226	7.1	7,280	5,155	1,147	98	264	434	8.4	33	12	1,917	56	386	1,280	0.2	512	3.E-03	−3.2	−21
	SD	1.3	0.2	119	2.0	855	734	183	28	52	89	2.3	5.7	3.1	345	17	118	306	0.03	86	8.E-04	0.6	3
	CV%	6	3	122	54	15	22	25	92	32	30	43	25	163	26	81	106	44	36	25	56	−14	−11

T: Temperature (°C), EC: Electrical conductivity (µS/cm); Eh (mV), P_{CO2} (atm), δ^{18}O and δD in per mille (‰) vs V-SMOW, TDS, O_2 and ionic concentrations in milligram per liter (mg/L). SD indicates the standard deviation and CV% the variation coefficient defined as 100 × SD / mean.

Figure 3 Dendrogram structure produced by the clustering procedure. Here the results of the unweighted pair-group average method (*UPGM*) of clustering are reported. Correlation coefficients were used as similarity coefficient.

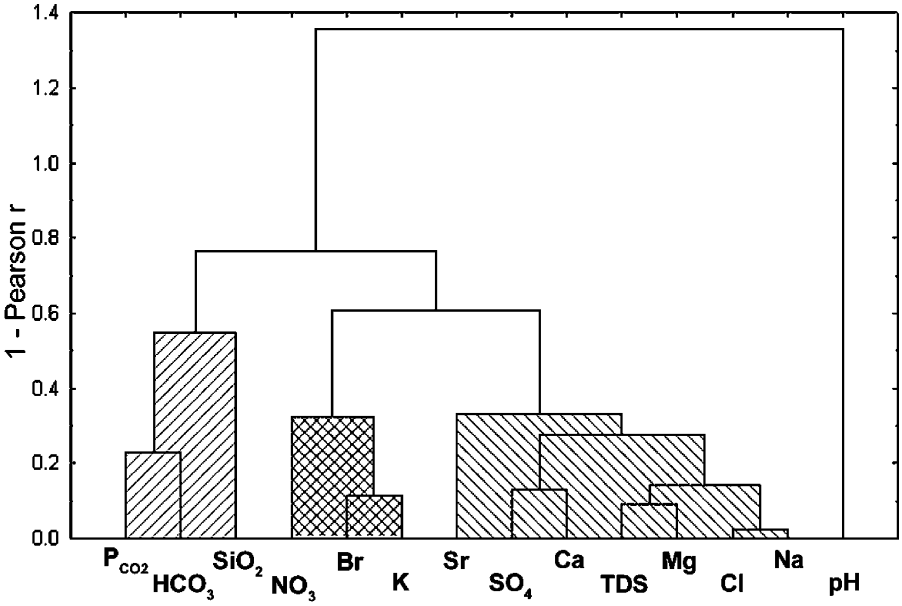

$r = 0.4$, three groups of related elements are identified. The first group includes TDS, Ca, Cl, Mg, Na, SO_4 and Sr, and reflects mineralization of groundwaters due to water–rock interactions. The highly significant relationships existing among major ions in solution and TDS, indicating that these ions tend to increase in concentration as water salinity increases. However, TDS is not highly correlated to pH, suggesting that the content of dissolved salts is not related to the acidic condition of groundwaters but result mainly from the dissolution of more soluble minerals. The contribution from dissolution of halite and gypsum is suggested by the strong correlations of SO_4 with Ca (0.87) and Cl with Na (0.98). In the second group, possible pollution of groundwaters by land use practices, including fumigation and pest-control treatments, cannot be ruled out, in view of the correlation between NO_3, K and Br. Nitrate concentrations in groundwaters are highly variable, ranging from 0.6 to 386 mg/L, with 50% of the analyzed samples exhibiting concentrations higher than 50 mg/L. This considerable variability is independent on groundwater salinity and suggests anthropogenic nitrate sources related to the land application of inorganic fertilizers. The third group reflects the known relationship between CO_2 dissolution and carbonate species (HCO_3) in solution. This group also includes SiO_2, which is negatively correlated with pH. Neither Na or Ca are significantly correlated with HCO_3. The lack of correlation between Ca and HCO_3 is probably due to a considerable dissolution of gypsum.

Table III Concentrations of major elements (mg/L) released during the leaching tests

		Na	K	Mg	Ca	Cl	SO_4	HCO_3
Calcarenites	S1	3.8	3.3	1.2	132	2.5	10	119
	S2	6.5	12	6.0	195	3.8	19	180
	S3	7.9	11	6.8	79	4.2	30	192
	S4	8.9	1.9	12	46	4.7	15	171
	S5	15	6.8	5.5	116	8.1	230	131
	S6	2.4	2.3	2.3	68	2.9	6.5	113
Clays	C1	28	33	66	200	9.9	373	110
	C2	8.1	11	25	307	5.7	26	110
	C3	2,440	180	243	581	2,087	3,682	204
	C4	290	44	87	258	610	227	521

3.3 Hydrogeochemical evolution of groundwaters along the flow path

The great variability in the chemical composition of the studied groundwaters may be explained by chemical processes of water–rock interaction. Groundwaters with EC < 1,700 μS/cm are dominated by Ca (>53% of total cations) and HCO_3 (>46% of total anions), thus indicating that carbonate rocks are the main reservoir for these waters. With increasing TDS, Na becomes the dominant cation (up to 46% and 60% of total cations in the second and third groups, respectively) and Cl and SO_4 increase their relative abundances. Leaching tests carried out to simulate leaching behaviour of the main local rocks confirm that the nature of the local substrate plays a dominant role in determining the chemical composition of groundwaters (Table III). Leaching of calcarenites essentially produces Ca–HCO_3 water types. Leaching of clays yields solutions of higher salinity, characterized by high concentrations of Na, Cl, Ca and SO_4 ions.

The Langelier and Ludwig's (1942) diagram (Figure 4) shows the distinct composition of groundwaters as a function of total salinity. Low-salinity waters (EC < 1,700 μS/cm) which probably represent the initial stage of underground circulation, start dissolving calcium carbonate from local rocks. The progressive increase in salinity, up to 4,400 μS/cm, accompanied by a change in water chemistry, now characterized by substantially higher Ca, SO_4, Na and Cl, suggests that dissolution of $CaSO_4$ and NaCl is an important process here. The further contribution of Na and Cl ions generates more saline waters (up to 7,280 μS/cm). During this step, the saturation index with respect to gypsum increases from −2.30 to −0.90, and precipitation of $CaCO_3$ may occur. Thus, the processes determining the observed water chemistry may be shown as:

$$CaCO_3 + H_2O + CO_2 \leftrightarrow Ca^{2+} + 2HCO_3^-$$

$$Ca^{2+} + 2HCO_3^- + CaSO_4 \cdot 2H_2O$$
$$\leftrightarrow CaCO_3 + Ca^{2+} + SO_4{}^{2-} + 3H_2O + CO_2$$

$$NaCl \leftrightarrow Na^+ + Cl^-$$

3.4 Isotope composition of local rainwaters and groundwaters

Hydrogen and oxygen stable isotope compositions of local rainwaters, surface and groundwaters are shown in Figure 5 using the conventional δ diagram. The $\delta^{18}O$

Figure 4 Langelier–Ludwing diagram for the study groundwaters.

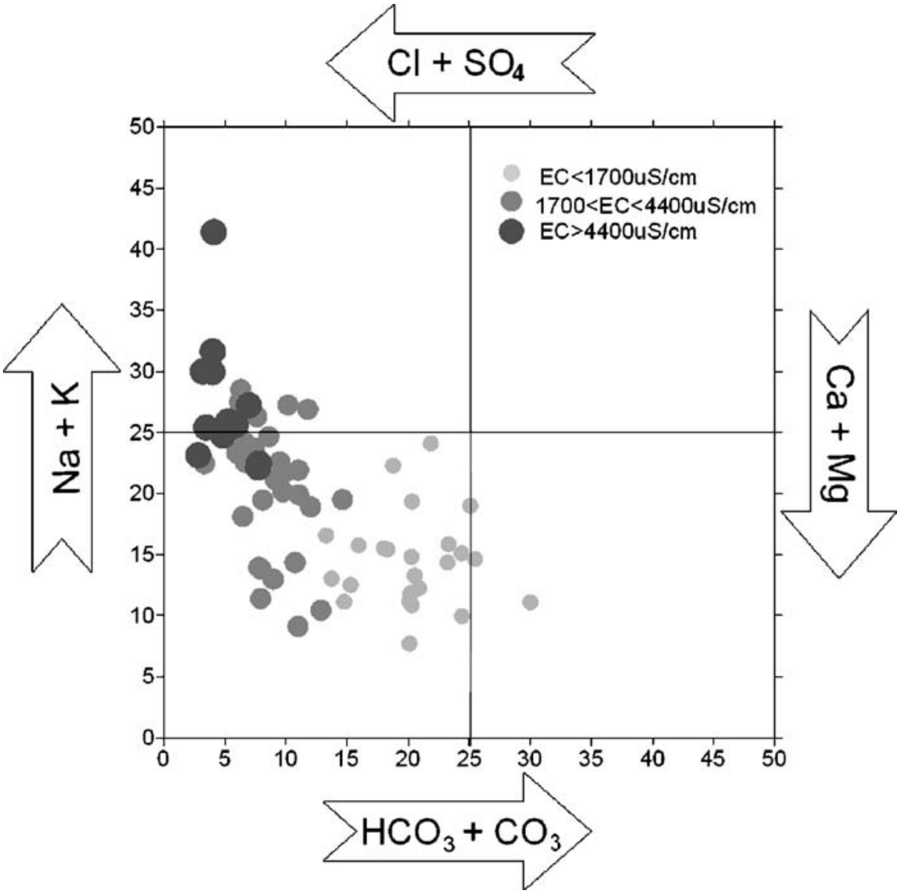

and δD values of water samples from local rainfall range from − 7.1‰ to −1.0‰ and from −38‰ to −6‰, respectively. They show typical seasonal variations, the more negative values being observed during winter. From an isotopic point of view, the heaviest rainfall was observed in August 2003 (δ^{18}O = −1.0‰ e δD = −6‰; average temperature 27°C) and the lightest in January 2005 (δ^{18}O = −7.1‰ e δD = −38‰; average temperature 13°C). The weighted average hydrogen and oxygen isotope signatures of rain samples were δ^{18}O = −5.5‰ and δD = −28‰.

These rainfall samples fall between the Global Meteoric Water Line (GMWL; Rozanski, Araguas-Araguas, & Gonfiantini, 1993) and the Mediterranean Meteoric Water Line (MMWL; Gat & Carmi, 1970) defining the following local meteoric water line (LMWL):

$$\delta\mathrm{D} = 5.6\ \delta^{18}\mathrm{O} + 2.0 \quad \left(r^2 = 0.99,\ n = 15\right)$$

The different slope and intercept with respect to GMWL and MMWL are consistent with non-equilibrium processes occurring after the condensation of water molecules from clouds. In dry environments, rain drops partly re-evaporate, acquiring a δ^{18}O/δD ratio generally in the range of 4–6, and an intercept close to 0 or negative (Gonfiantini, 1986). At an environmental temperature of 20°C, the intercept is about 4 (Jouzel, 1986). Ayalon, Bar-Matthews, and Sass (1998) found that, in the Mediterranean area, the relationship between δ^{18}O and δD is a function of the amount of rainfall: heavy rain is characterized by the highest excess of deuterium and a slope close to 8, whereas rainfalls of less than 10 mm have lower d-excess values and a slope <8. For the Hyblean area, close to the present study area, Grassa (2002) reported a trend with a slope of 6.14 and an intercept of 6.8.

The δ^{18}O and δD compositions of the analysed groundwaters range from −6.1‰ to −1.5‰ and from −38‰ to −12‰, respectively. The average values (δ^{18}O = −4.9‰ and δD = −29‰), within the range for local rains, are consistent with the meteoric origin of groundwaters. They also reflect the greater contribution of autumn and winter precipitations (more than 90%) to the recharge. Most of the groundwater samples plot on the right of the local meteoric water

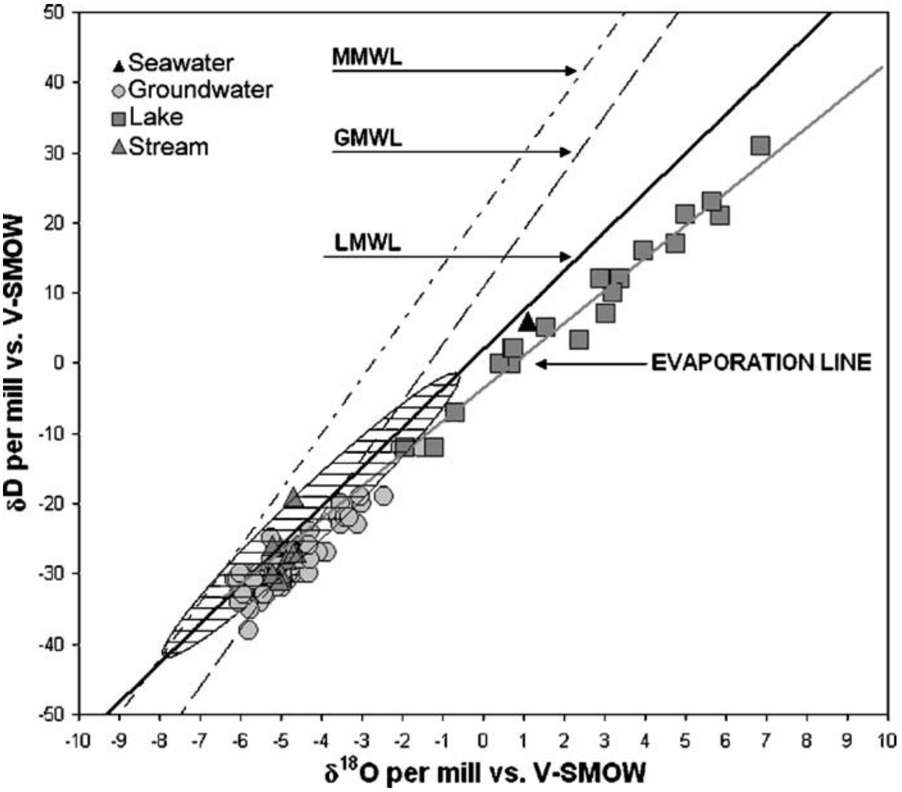

Figure 5 δD–δ^{18}O relationship in rain and groundwater samples. The Mediterranean Meteoric Water Line [MMWL; (Gat & Carmi, 1970)], the Global Meteoric Water Line [GMWL; (Rozanski et al., 1993)] and the Local Metoric Water Line (LMWL) are also reported. The dashed area shows the isotope compositions of local rainfall samples.

Table IV Physico-chemical parameters and element concentrations in lake waters

	Date	T	pH	Eh	O_2	EC	TDS	Na	K	Mg	Ca	Sr	SiO_2	F	Cl	Br	NO_3	SO_4	CO_3	HCO_3	P_{CO2}	$\delta^{18}O$	δD
"Lago Grande"	Jul 03	30	8.1	nd	nd	4,170	2,735	486	17	100	298	5.9	3.8	1.2	806	1.7	1.0	899	0.4	111	2E-05	2.4	3
	Nov 03	19	8.3	nd	nd	4,770	3,855	693	37	140	355	6.4	4.1	1.2	1,465	11	2.2	1,033	0.5	103	2E-05	3.4	12
	Jan 04	10	8.0	220	nd	2,930	2,005	343	14	45	226	4.6	7.8	0.7	613	6.2	3.9	577	0.0	148	6E-05	−1.9	−12
	Mar 04	13	7.9	215	6.8	3,250	2,041	336	13	51	224	4.7	4.6	0.8	513	7.3	3.0	654	0.3	141	6E-05	−1.1	−23
	Apr 04	17	8.2	128	8.2	3,400	2,228	367	16	88	242	3.8	3.9	1.0	564	6.0	1.0	701	0.5	135	3E-05	−0.7	−7
	Jun 04	23	8.1	93	7.9	3,530	1,720	378	15	82	253	4.8	0.5	1.0	589	0.1	25	747	0.4	135	7E-05	0.7	0
	Jul 04	31	8.4	125	13	3,860	1,905	410	22	108	263	5.2	0.6	11	707	6.5	24	805	0.7	110	2E-05	3.0	7
	Aug 04	30	8.4	129	15	4,080	2,198	500	20	142	324	5.5	0.7	11	816	6.3	21	924	0.5	90	2E-05	3.2	10
	Oct 04	24	8.4	nd	9.8	4,320	1,906	502	21	133	275	5.4	0.6	0.9	878	12	1.0	907	0.4	54	1E-05	4.0	16
	Nov 04	15	8.7	226	9.0	2,830	1,339	296	14	93	196	4.2	0.4	1.3	531	5.7	6.7	646	0.8	65	7E-06	−1.2	−12
	Feb 05	9.6	7.1	186	7.5	1,572	827	147	12	44	149	3.6	0.3	0.4	264	2.8	9.7	310	0.0	152	1E-03	−4.8	−25
"Lago Piccolo"	Jul 03	29	8.1	nd	nd	6,525	4,473	879	28	165	473	8.8	3.3	1.9	1,436	2.5	11	1,371	0.3	94	2E05	5.0	21
	Nov 03	19	8.4	240	nd	9,440	7,856	1,678	56	298	674	10	0.3	1.8	2,913	20	5.3	2,099	0.7	110	1E-05	5.8	21
	Jan 04	10	8.5	210	nd	6,250	4,576	849	21	152	398	8.2	3.5	0.7	1,535	12	2.7	1,485	0.0	108	1E-05	0.4	0
	Mar 04	13	7.9	223	6.2	6,300	3,873	779	26	182	353	7.2	3.7	1.2	1,210	16	4.3	1,084	0.2	131	6E-05	0.7	2
	Apr 04	17	8.3	143	9.0	6,520	4,283	833	38	172	391	8.0	3.8	1.4	1,398	10	1.0	1,199	0.6	119	2E-05	1.6	5
	Jun 04	24	7.8	90	7.3	6,970	3,109	904	22	172	419	7.7	0.9	1.7	1,559	0.1	30	1,352	0.2	129	1E-04	2.9	12
	Jul 04	30	7.8	148	7.3	8,130	3,468	997	35	242	476	7.9	1.0	18	1,736	14	49	1,435	0.2	122	1E-04	4.8	17
	Aug 04	29	8.2	121	8.8	8,850	3,894	1,175	39	290	533	8.1	1.1	22	1,954	8.2	49	1,583	0.1	97	3E-05	5.6	23
	Oct 04	25	8.1	nd	8.8	10,820	4,961	1,469	40	381	638	9.6	1.4	1.3	3,110	25	1.0	2,316	0.3	91	3E-05	6.8	31
	Nov 04	16	8.4	174	8.2	6,380	2,745	800	29	236	374	7.5	0.8	10	1,494	24	1.0	1,179	0.6	84	2E-05	0.8	2
	Feb 05	9.0	7.3	212	8.2	1,613	845	126	9.1	45	153	4.5	0.3	0.6	222	1.1	6.3	336	0.1	168	7E-04	−4.5	−25

T: Temperature (°C), EC: Electrical conductivity (μS/cm); Eh (mV), P_{CO2} (atm), $\delta^{18}O$ and δD in per mille (‰) vs V-SMOW, TDS, O_2 and ionic concentrations in milligram per liter (mg/l).

line (LMWL), describing the following least-square linear regression ($r^2 = 0.82$, $n = 128$):

$$\delta D = 4.5\ \delta^{18}O - 7.3$$

Enrichment in ^{18}O and D with respect to local precipitations suggests evaporation effects, which are higher in valleys, where the water table is shallower. In addition, the less saline waters are less enriched in heavy isotopes, with δ^{18}O values between −5.7 and −4.8‰ and δD between −34 and −30‰, pointing to lower evaporation.

3.5 Geochemistry of the lake water

During the study period the “Biviere di Gela” lake showed a quite good vertical mixing within the water column, even when the lake itself had subdivided into two distinct water bodies. Only a slight variation in dissolved O_2 with depth was observed. Table IV lists the physical and chemical variables of the two water bodies. “Lago Grande” water is generally of Na-SO_4-Cl-type, whereas “Lago Piccolo” water is of Na-Cl-SO_4-type. TDS exhibit considerable variations over time and, except in February 2005, the “Lago Piccolo” always had higher values. This reflects its smaller volume and the sporadic input of water from an artificial canal into “Lago Grande”. pH and total alkalinity range between 7.1-8.4 and 54-168 mg/L, respectively. Langelier–Ludwig's diagram shows that the analysed samples fall in the chloride–sulphate–alkaline and chloride–sulphate–earth alkaline fields. With respect to “Lago Grande,” taking into account previous data and the results of this study, there is an increasing trend towards greater salinity and also changes in the relative abundances of Cl and SO_4 (Figure 6). These chemical changes are probably due to the contribution of sulphate dominant water from the Ficuzza–Dirillo canal (Table I). Nitrate concentrations in lake waters are generally lower than average nitrate in groundwaters and similar to those observed in stream waters. The highest concentrations are observed during summertime, when the contribution of groundwaters, which contain high levels of nitrate, becomes predominant.

Waters from both “Lago Grande” and “Lago Piccolo” undergo substantial fluctuations in hydrogen and oxygen isotope compositions during the annual cycle, due to seasonality in the water budget and

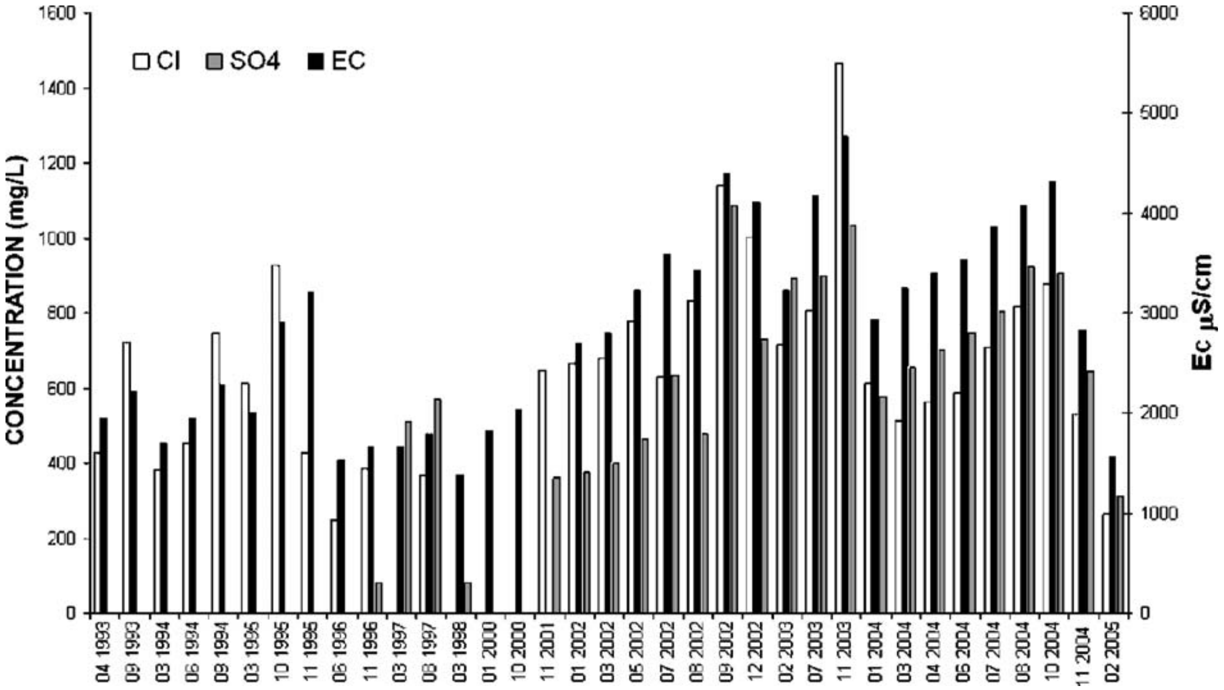

Figure 6 Temporal variations of some physico-chemical (*EC*) and chemical parameters (Cl and SO_4). Chemical data previous to July 2003 furnished by the Riserva Naturale Orientata “Biviere di Gela.”

evaporative effects. The isotope data define a straight line (Figure 5) with regression equation:

$$\delta\mathrm{D} = 5.0\,\delta^{18}\mathrm{O} - 5.2 \quad \left(r^2 = 0.92,\ n = 21\right)$$

The extent of these fluctuations is controlled by metereological variables, such as relative atmospheric humidity, lake water temperature and the ratio of evaporation to inflow.

The δ^{18}O/Cl diagram (Figure 7) was used to model the evolving chemical and isotopic composition of lake waters, starting from local groundwaters. The diagram also shows the theoretical mixing line between groundwater and seawater.

The lake waters plot on the right of the mixing line, thus excluding the direct contribution of seawater. The stable isotope evolution of lake waters during the annual evaporation cycle was established in its main principles using the Craig–Gordon model (Craig & Gordon, 1965), which takes into account fluctuations in lake water volumes due to evaporation, equilibrium and kinetic fractionation factors, and the effect of changing seasonal temperatures and humidity. Here, the degree of isotope enrichment due to evaporation was calculated from the following equation (Gonfiantini, 1986):

$$d\delta/d\ln f = [h(\delta - \delta_a) - (\delta + 1)(\Delta\varepsilon + \varepsilon/\alpha)]/[1 - h + \Delta\varepsilon]$$

which describes variations in isotopic composition as the residual liquid fraction (*f*) decreases. In the above equation, δa is the δ^{18}O of atmospheric water vapour, *h* the fractional relative humidity, ε the equilibrium enrichment factor, α the isotope liquid-vapour fractionation factor, and Δε the additional diffusive (kinetic) isotope fractionation, which results from the separate diffusivity of isotopically different water molecules at the liquid–air boundary. The observed evaporation lines fit a Raleigh-type evaporative process with relative humidity of approximately 70%–75%, in agreement with meteorological data, confirming that evaporation controls chemical and isotopic compositions.

3.6 "Lago Grande" water budget

Isotope and geochemical data were used to derive the mixing proportions of lake and inflow waters. This may be of importance in predicting the geochemical evolution of the lake and planning adequate management strategies for its conservation.

Heavy isotope enrichment ($\delta^{18}O_L$= 3.4‰) peaks at the end of summer, during October–November whereas waters become depleted in heavy isotopes during late autumn and winter, with a minimum in January–February ($\delta^{18}O_L$= −1.9‰).

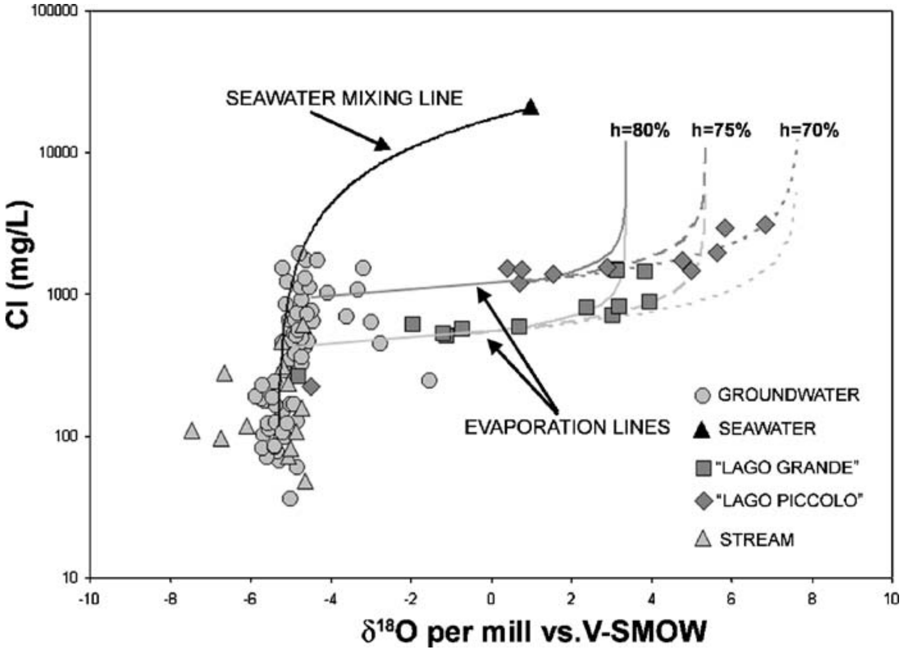

Figure 7 δ^{18}O-chloride relationship in lake and groundwater samples. Evaporation curves, computed for different relative humidities (*h*), and the theoretical mixing line with seawater are also reported. The δ^{18}O value of atmospheric vapour is assumed to be 12‰.

The amount of inflow during November–January may be estimated by the following equation:

$$\delta^{18}\mathrm{O}_{\mathrm{L(November)}}(1-X)+\delta^{18}\mathrm{O}_{\mathrm{I}}(X)=\delta^{18}\mathrm{O}_{\mathrm{L(January)}}$$

where X is the percentual contribution of inflowing water and subscripts I and L refer to inflow and lake, respectively. The assumptions made here are that the isotope signature of the inflow is identical to the average isotopic composition of groundwaters ($\delta^{18}O_G$ = −4.9‰) and that the evaporation rate is negligible during the same period. According to the above equation, an inflow of about 64% of fresh water was computed.

A combination of this value and chemical data allow us to estimate the chemical composition of the feed water. The following mass balance equations can be formulated:

$$\mathrm{Cl}_{\mathrm{L(November)}}(1-0.64)+0.64Y_{\mathrm{Cl}}=\mathrm{Cl}_{\mathrm{L(January)}}$$
$$\mathrm{SO}_{4\mathrm{L(November)}}(1-X)+Y_{\mathrm{SO4}}(X)=\mathrm{SO}_{4\mathrm{L(January)}}$$

where Y_{Cl} and Y_{SO4} indicate chloride and sulphate concentrations in inflowing waters. It was found that the lake is fed primarily by low-salinity water, with SO_4 (~321 mg/L)>Cl (~134 mg/L). In the study area, low-salinity waters with SO_4 higher than Cl are those from surface runoff; thus, it may be concluded that runoff is the main feeder of the lake. Such a dependence on the contribution of surface runoff explains the changes in the chemical composition of "Lago Grande" water, from Cl-dominant (until 12/2002) to SO_4-dominant (since 02/2003) (Figure 6). This finding also fits the results of the hydrogeological mass balance (see Section 2.2).

3.7 Trace elements in lake waters and bottom sediments

Trace metal (As, Cd, Cr, Mn, Ni, Se, Zn,) concentrations were determined in lake waters and sediments (Table V). "Lago Piccolo" water generally contains higher concentrations of these elements. As, Ni and Se in waters vary positively with TDS, as shown by their significant correlation coefficients (0.68, 0.69 and 0.70 for As, Ni and Se, respectively). Thus, their variability is strictly related to the runoff input during the wet season and to evaporation during the dry season. On the other hand, Cd, Cr, Mn and Zn appear to be almost independent on seasons. With respect to the guidelines reported by the Italian D.M. 471/99 (Gazzetta Ufficiale della Repubblica Italiana (GURI), 1999), Mn concentrations in both lakes are always higher than the permissible levels, whereas As, Ni and Se exceed the limits only occasionally.

Metal concentrations in the analysed sediments were compared with ERL (Effects Range-Low) and ERM (Effects Range-Median) guideline values (Long, MacDonald, Smith, & Calder, 1995) and with the guidelines listed in the Italian D.M. 367/2003 (Gazzetta Ufficiale della Repubblica Italiana (GURI), 2004). ERL and ERM values, respectively, represent concentrations below which adverse effects are rarely observed and above which effects frequently occur. Among the trace elements determined here, As (20–31 mg/kg), Cd (0.4–0.8 mg/kg), Cr (45–78 mg/kg) and Ni (26–34 mg/kg) exceed the screening levels set by DM 367/2003 (Gazzetta Ufficiale della Repubblica Italiana (GURI), 2004) at selected locations. As and Ni also exceed the ERL values, but are lower than the ERM, according to Long et al. (1995) the incidence of adverse biological effects may be predicted to increase by 20%–30%.

4 Conclusions

Water–rock interactions produce at least three different types of waters in the study area. Waters of predominantly $Ca(HCO_3)_2$ character, representing the initial stage of underground circulation, are found in areas of local recharge. In topographically flat areas, leaching of soluble evaporitic salts and slight evaporation change the chemical composition of waters from HCO_3-dominant to SO4-dominant. NaCl-type waters characterize lower-lying areas. Surface and ground waters are vulnerable to pollution from land use in the recharge catchment area. Except in the case of a few wells along the coast, mixing with seawater does not appear to be a main source of groundwater mineralization.

"Lago Grande" water is generally of Na–SO_4–Cl-type, whereas "Lago Piccolo" water is of Na–Cl–SO_4-type. Their total content of dissolved salts varies with season, the amount of rainfall, and inflow of ground and drainage water. Over time, an increasing trend towards greater salinity and also sudden changes in the relative abundances of Cl and SO_4 have been

Table V Trace element concentrations in lake waters (μg/L) and in bottom sediments (mg/kg). nd = not determined

	"Lago Grande"								"Lago Piccolo"						
	Date	As	Cd	Cr	Mn	Ni	Se	Zn	As	Cd	Cr	Mn	Ni	Se	Zn
Waters	Jul 03	6.6	0.005	0.0	191	3.6	5.0	4.5	6.9	0.004	0.9	751	9.6	13	6.7
	Mar 04	9.1	0.005	0.1	213	6.9	5.9	13	16	0.004	0.1	484	7.3	11	14
	Apr 04	2.4	0.005	0.1	420	7.1	3.8	5.7	1.2	0.004	1.8	298	7.6	20	5.9
	Jun 04	3.0	0.005	0.1	681	9.0	1.8	2.3	5.4	0.004	0.1	810	12	3.2	2.3
	Jul 04	4.9	0.008	0.7	187	12	4.6	8.6	9.8	0.039	2.0	851	22	11	15
	Aug 04	6.2	0.024	0.7	205	12	4.6	8.4	3.6	0.015	0.9	856	16	4.9	13
	Oct 04	7.3	0.018	0.8	230	13	5.9	10	16	0.064	2.4	925	31	16	19
	Nov 04	4.1	0.025	0.6	350	10	3.3	8.8	6.1	0.027	1.6	916	20	8.8	13
Sediments		26	0.4	47	1,194	26	nd	40	21	0.8	73	1,979	32	nd	70
		20	0.7	45	1,072	27	nd	45	31	0.7	78	1,098	34	nd	79

recorded for the "Lago Grande." The chemical and isotopic compositions of the water appear to be affected by several factors:

1) inflow of ground and surface waters with a geochemical signature derived from mineral weathering reactions in the catchment area; according to chemical and isotopic data, runoff is the main feeder;
2) evaporative loss: stable isotope data are consistent with Raleigh-type evaporation occurring at relative humidity of 70%–75%;

It is also worth to note the elevated nitrate levels in waters, revealing the effects of intensive agricultural production. The observed high content of nitrate in lake waters arises particular concerns because it can contribute to algal blooms and eutrophication.

Finally, the results of this study do not evidence the presence of any significant metal contamination of lake waters and although the risk of metal accumulation might not be felt for some time to come, a future potential hazard of metals bioaccumulation by the aquatic biota cannot be disregarded.

The lake water balance indicates that a drop in local precipitation of about 20% would become critical in maintaining the present water level and might be critical for lake survival. Moreover, in summer the lake feeds the water table. Therefore, the results of the present survey indicate the need to be aware of the quality and quantity of water inflows, and also to estimate the amount of withdrawal from nearby wells, in order to sustain the delicate environmental balance of the "Biviere di Gela" lake and its related ecosystems.

Acknowledgment The survey was financially supported by funds MIUR ex 60%.

References

Ayalon, A., Bar-Matthews, M., & Sass, E. (1998). Rainfall–recharge relationships within a karstic terrain in the eastern Mediterranean semi-arid region, Israel: δ^{18}O and δD characteristics. *Journal of Hydrolology*, *207*, 18–31.

Ball, J. W., & Nordstrom, D. K. (1991). User's manual for WATEQ4F, with revised thermodynamic data base and test cases for calculation speciation of major, trace, and redox elements in natural waters, US Geological Survey, Open File Report 91–193, 189.

Beneo, E. (1949). Sul "Microdiapiro" di Leonforte e su quelli a Nord di Gela (Sicilia Centrale e Meridionale). *Rend. Acc. Lincei.*, *7*(1–4), 108–113.

Butler, R. W. H., Grasso, M., & Lickorish, H. (1995a). Plio-quaternary megasequence geometry and its tectonic control within the Maghrebian thrust belt of south-central Sicily. *Terra Nova*, *7*, 171–178.

Butler, R. W. H., Lickorish, W. H., Grasso, M., Pedley, H. M., & Ramberti, L. (1995b). Tectonics and sequence stratigraphy in Messinian basins, Sicily: Constraints on the initiation and termination of the Mediterranean salinity crisis. *Geological Society of American Bulletin*, *107*, 425–439.

Butler, R. W. H., McClelland, E., & Jones, R. E. (1999). Calibrating the duration and timing of the Messinian salinity crisis in the Mediterranean: Linked tectonoclimatic signals in thrust-top basins of Sicily. *Journal of the Geological Society (London)*, *56*, 827–835.

Craig, H., & Gordon, L. I. (1965). Deuterium and oxygen-18 variations in the ocean and marine atmosphere. In E. Tongiorgi (Ed.), *Stable Isotopes in Oceanographic Studies* *and Paleo-Temperatures, Pisa* (pp. 9–130). Lab. Geol. Nucl.

De Martonne, E. (1926). Une nouvelle function climatologique: L'indice d'ariditè. *Meterologie*, *2*, 449–459.

Gat, J. R., & Carmi, I. (1970). Evolution of the isotopic composition of atmospheric water in the Mediterranean Sea area. *Journal of Geophysical Research*, *75*, 3039–3048.

Gonfiantini, R. (1986). Environmental isotopes in lake studies. In P. Fritz & J. Ch. Fontes (Eds.), *Hanbook of Environmental Isotopes Geochemistry*, vol. 2, B (pp. 113–168), Amsterdam: Elsevier.

Grassa, F. (2002). Geochemical processes governing the chemistry of groundwater hosted within the Hyblean aquifers (South-Eastern Sicily, Italy). Ph.D. thesis, Dipartimento di Chimica e Fisica della Terra (CFTA), University of Palermo, 80 pp.

GreenStream, S. P. A. (2003). Progetto di realizzazione del metanodotto di importazione dalla Libia. Procedura VIA. Piano di gestione monitoraggio e di ricerca dell'area SIC "Biviere e Macconi di Gela" e riqualificazione dell'ambito dunale, pp. 465.

Gazzetta Ufficiale della Repubblica Italiana (GURI) (1999). Decreto Ministeriale 25 ottobre 1999, n. 471 – Regolamento recante criteri, procedure e modalità per la messa in sicurezza, la bonifica e il ripristino ambientale dei siti inquinati, ai sensi dell'articolo 17 del decreto legislativo 5 febbraio 1997, n. 22, e successive modificazioni e integrazioni.

Gazzetta Ufficiale della Repubblica Italiana (GURI) (2004). Decreto Ministeriale 6 novembre 2003, n° 367. Regolamento concernente la fissazione di standard di qualità nell'ambiente acquatico per le sostanze pericolose, ai sensi dell'articolo 3, comma 4, del decreto legislativo 11 maggio 1999, n. 152. Ministero dell'Ambiente e della Tutela del Territorio, Roma, 08 Gennaio 2004, 5, 17–29.

ISTAT (2000). Censimento generale dell'agricoltura, http://www.istat.it.

Jouzel, J. (1986). Isotopes in cloud physics: Multiphase and multistage condensation processes. *Handbook of Enviromental Isotopes Geochemistry*, *2*, 61–112.

Langelier, W. F., & Ludwig, F. (1942). Graphical methods for indicating the mineral character of natural waters. *Journal of the American Water Works Association*, *34*, 335–352.

Long, E. R., MacDonald, D. D., Smith, S. L., & Calder, F. D. (1995). Incidence of adverse biological effects within ranges of chemical concentrations in marine and estuarine sediments. *Environmental Management*, *19*(1), 81–97.

Pedley, H., & Grasso, M. (1991). Sea-level change around the margins of Catania-Gela through and Hyblean Plateau, southeast Sicily (African–European plate convergence zone): A problem of Plio-Quaternary plate buoyancy. *Special Publication of the International Association of Sedimentologists*, *12*, 451–464.

Roda, C. (1966). Nuove conoscenze sulla trasgressione mediopliocenica. *Bollettino dell'Accademia Gioenia di Scienze Naturali*, *8*, 705–716.

Rozanski, K., Araguas-Araguas, L., & Gonfiantini, R. (1993). Isotopic patterns in modern global precipitation. In P. K. Swart, K. C. Lohmann, J. McKenzie, & S. Savin (Eds.), *Climate Change in Continental Isotopic Records* (pp. 1–36), Geophysical Monograph 78, American Geophysical Union.

Servizio Idrografico del Genio Civile. Annali idrologici Parte II, Regione Siciliana Ed. Palermo, (1980–2000) http://www.uirsicilia.it/.

Tennant, C. B., & White, M. L. (1959). Study of the distribution of some geochemical data. *Economic Geology*, *54*, 1281–1290.

Thornthwaite, C. W. (1948). An approach towards a rational classification of climate. *Geographical Review*, *38*, 85–94.